Astronomical and Astrophysical Transactions (*AApTr*), 2017, Vol. 30, Issue 2, pp. 241–248,
ISSN 1055-6796, Photocopying permitted by license only, ©Cambridge Scientific Publishers

Toward the birth of very wide binary stars

S.N. Zamozdra*, N.S. Kargaltseva

Chelyabinsk State University, Br. Kashirinykh Str., 129, Chelyabinsk, 454001, Russia

During initial (quasi-isothermal) collapse stage of protostellar clouds the magnetosonic pulsations become gravitationally unstable when density increases at 2–3 orders of magnitude. If the region of such density has supercritical ratio of rotational to gravitational energies: $\varepsilon_{\rm rot} \gtrsim 0.14$–$0.27$, then fragmentation occurs. Such early fragmentation causes a large separation between protostars and can be formation mechanism of wide binary or multiple stars. The rotation of cloud central region is the superposition of cloud rotation and turbulent motion. If these motions are codirectional then supercritical values of $\varepsilon_{\rm rot}$ are more probable, otherwise – less probable. During 3D MHD simulations we found the cases when only 1/7 of realizations of initial turbulence lead to early fragmentation. In some cases the ratio of fragments separation d to initial cloud radius can achieve 0.4 that corresponds to very wide binaries: $d \approx 10^3$–10^4 AU.

Keywords: Stars: binaries: general – stars: formation – stars: protostars

1 Introduction

Zinnecker (1984) suggested the classification of binary stars by periods, P (Table 1). However there is no generally accepted terminology in this data domain.

For example, Brandner and Kohler (1998), Allen and Monroy-Rodriguez (2014) use the term "wide binary" for systems with projected separations $d > 50$ and $d > 100$ AU, respectively. In Longhitano and Binggeli (2010) "wide" systems have $P = 10^3$–10^6 yr, and "very wide" systems have $d > 0.1$ pc. Kraus and Hillenbrand (2009) call "wide" the systems with $d = 500$–5000 AU. For Chen et al. (2013) wide binary protostars begin from $d = 1000$ AU, while for Kaib and Raymond (2014) it is minimal separation for "very wide" stars.

For Connelley et al. (2008) wide systems have angular separation $>1''$. In Scholz et al. (2008) "extremely wide" binaries have angular separation $>1^\circ$.

These examples show the tendency to the stretching of three last intervals in Table 1 towards higher values because of growing statistics of wider systems. Indeed, in Zinnecker's (1984) work the most frequent period among 76 systems is 14 yr that corresponds to $d = 6$ AU at sum component mass 1.5 $M_\odot$. Raghavan et al. (2010) for 259

*Email: sezam@csu.ru

Table 1 Zinnecker's (1984) classification of binary stars by periods. We computed the correspondent intervals of major semi-axis at sum component mass 1.5 $M_\odot$ as Raghavan et al. (2010).

Class	Period, yr	Major semi-axis, AU
Contact	$<10^{-3}$	<0.01
Very close	10^{-3}–1	0.01–1
Close	1–10	1–5
Wide	10–100	5–23
Very wide	100–10^3	23–100
Extremely wide	$>10^3$	>100

pairs obtained most frequent period 10^4–10^5 days that means $d = 10$–50 AU. Longhitano and Binggeli (2010) calculated angular two-point correlation function from a homogeneous sample of nearly 670000 main sequence stars and found most frequent $d \approx 6000$ AU.

Of course, weakly bound binaries have low stability. Kraus and Hillenbrand (2009) showed that "higher mass stars have a higher frequency of wide binary companions, and there is a marked paucity of wide binary systems near the substellar regime". Raghavan et al. (2010) confirmed: "bluer, more massive stars are seen as more likely to have companions than redder, less massive ones".

Modern sub-millimeter observations give data about binary and multiple protostars. 67 Class I protostellar systems considered by Connelley et al. (2008) have $d = 500$–4500 AU. The median separation decreases at 1/5 during the Class I phase; binary frequency remains constant until the end of the Class I phase, when it drops sharply. 21 Class 0 protostellar systems in the sample of Chen et al. (2013) have $d = 50$–5600 AU. Half of these systems have $d \simeq 1000$ AU. Chen et al. (2013) concluded that multiplicity decreases from Class 0 (≈ 0.63) to Class I ($\approx$0.35) and to main sequence ($\approx$0.2).

Zinnecker (1984) divided 5 mechanisms of binary formation. For spectroscopic (close) binaries it is 1) fragmentation of collapsing clouds or 2) accretion disks and 3) fission of quasi-static protostars. For visual (wide) binaries it is 4) mutual gravitational capture of protostars and 5) disintegration of small clusters.

Modern numerical models of collapse and fragmentation of prestellar cores of molecular clouds (hereafter, *protostellar clouds*) show that separation between fragments can exceed 100 AU, i.e. such fragmentation explains the origin both of close and wide binaries. For example, in the model of Burzle et al. (2011) rapidly rotating not turbulent protostellar cloud with radius $R_0 = 2666$ AU generates protostars with separation $d = 40$–400 AU. In the model of Joos et al. (2013) slowly rotating turbulent protostellar cloud with $R_0 = 28877$ AU generates protostars with $d = 200$–500 AU.

In these examples $d/R_0 = 0.009$–0.15. In the present work we show that the ratio d/R_0 may be even more if both moderate rotation and strong turbulence present in a protostellar cloud. We also point out that turbulence can prevent fragmentation of a rotating cloud if during a critical evolution stage the turbulent and rotational motions in cloud center are oppositely directed.

2 Model and methods

We investigate the combined influence of thermal pressure, magnetic field, turbulence and rotation on the collapse and fragmentation of protostellar clouds in the approximation of ideal magnetohydrodynamics (MHD). The basic form of MHD equations is:

$$\frac{\partial \rho}{\partial t} = -\nabla(\rho \mathbf{v}) \ , \tag{1}$$

$$\rho \left(\frac{\partial \mathbf{v}}{\partial t} + (\mathbf{v}\nabla)\mathbf{v} \right) = -\nabla p + \frac{1}{4\pi} (\nabla \times \mathbf{B}) \times \mathbf{B} - \rho \nabla \Phi \ , \tag{2}$$

$$\frac{\partial \mathbf{B}}{\partial t} = \nabla \times (\mathbf{v} \times \mathbf{B}) \ , \tag{3}$$

$$\frac{\partial p}{\partial t} = -\nabla(p\mathbf{v}) \ , \tag{4}$$

$$\nabla^2 \Phi = 4\pi G \rho \ , \tag{5}$$

where ρ – density, $\mathbf{v}$ – velocity, $\mathbf{B}$ – magnetic induction, p – pressure, Φ – gravitational potential.

Equation (4) describes the pressure evolution in flows with invariable temperature of individual particles. This approximation is applicable for the modelling of initial collapse of protostellar clouds (density contrast $< 10^4$) when the gas-dust medium is transparent to own thermal emission. Indeed, complicated 3D MHD models of protostars formation which include the full gas-grain chemistry and radiation transfer (Hincelin et al. 2016) show that the medium with H_2 density $< 10^9$ cm^{-3} have temperature 10–30 K. Such the temperature variations are negligible in comparison with density variations.

Equations (1–5) are transformed to dimensionless form and are written in Cartesian coordinates. The hyperbolic subsystem (1–4) is converted to conservative form. 3D problem with initial and boundary conditions for this subsystem is solved numerically by grid method of Lax–Friedrichs type (Dudorov et al. 1999). 3D problem for Poisson equation (5) is solved numerically by the method of conjugated gradients. All these methods are realized in program code Megalion (Dudorov et al. 2003) in joint with adaptive mesh refinement (AMR) technology. The AMR is controlled via condition that cell size must be less than the critical length of gravitationally unstable perturbations.

Initial conditions are the following. Spherical cloud with radius $R_0 = 0.3L$ and uniform density $\rho_0 = 1$ is embedded into cubic medium with size L and uniform density $0.25\rho_0$. External and internal pressures are balanced. Large scale magnetic field $\mathbf{B}_0$ is uniform. The cloud and medium can rotate as solid body with axis parallel to $\mathbf{B}_0$. Turbulence is the ensemble of plane harmonic Alfven waves with linear polarization and isotropic power law spectrum. The initial velocity pulsation $\mathbf{v_k}$ in the Alfven wave with wave vector $\mathbf{k}$ is directed perpendicularly to $(\mathbf{k}, \mathbf{B}_0)$ plane and has amplitude

$$v_{\mathbf{k}}(\mathbf{r}) = A|\mathbf{k}|^{-\alpha} \rho^{\beta}(\mathbf{r}) \sin(\mathbf{kr} + \varphi_{\mathbf{k}}) \ , \tag{6}$$

where A is the normalization factor, $\alpha = 1/3$ and $\beta = -1/2$ are parameters, $\varphi_{\mathbf{k}}$ is the random phase. The magnetic pulsation is $\mathbf{B_k} = \mp s \mathbf{v_k} \sqrt{\rho}$, where $s = sign(\mathbf{kB}_0)$.

The values of pressure, angular velocity, B_0 and A are calculated via the ratios of thermal, rotational, magnetic and turbulent kinetic energies to the absolute value of gravitational energy of the cloud: $\varepsilon_{\rm T}$, ε_{Ω}, $\varepsilon_{\rm M}$, $\varepsilon_{\rm tk}$, respectively. Different realizations of turbulence can have the same $\varepsilon_{\rm tk}$ due to fitted A. $n_{\rm max} = 8$ and $n_{\rm min} = 2$ are the numbers of shortest and longest waves that fit on the length L.

Periodical boundary conditions are used for equations (1)–(4) to promote the MHD waves circulation through the medium.

3 Results

We look for clumps in the density field and calculate their characteristics in order to select the fragments of the cloud. We define a *clump* as a set of contacting cells in which the density exceeds some limiting value. In order to estimate the gravitational connectivity of a clump we consider gas motions relative the mass center of the clump and take only the internal motions and interactions into account. The flows directed to the clump center promote the collapse (Hunter 1979), therefore we say that clump is bound if

$$-E_{\rm in} + E_{\rm out} + E_{\rm tan} + E_{\rm t} + E_{\rm m} - E_{\rm g} < 0\,, \qquad (7)$$

where $E_{\rm in}$, $E_{\rm out}$, $E_{\rm tan}$ are the energies of centripetal, centrifugal and tangential motions of the gas, $E_{\rm t}$ and $E_{\rm m}$ are thermal and magnetic energies of the clump, $E_{\rm g}$ is the absolute value of its gravitational energy.

We define the *fragmentation* as the appearance of two or more *fragments* – self-gravitating clumps fulfilling the criterion (7).

During initial (quasi-isothermal) collapse stage of protostellar clouds the magnetosonic pulsations become gravitationally unstable when density increases at 2–3 orders of magnitude (Dudorov and Zamozdra 2012). It happens because Alfven velocity is almost constant during this collapse stage. If the region of such density has supercritical ratio of rotational to gravitational energies: $\varepsilon_{\rm rot} \gtrsim 0.14$–$0.27$, then fragmentation occurs (Dudorov and Zamozdra 2013).

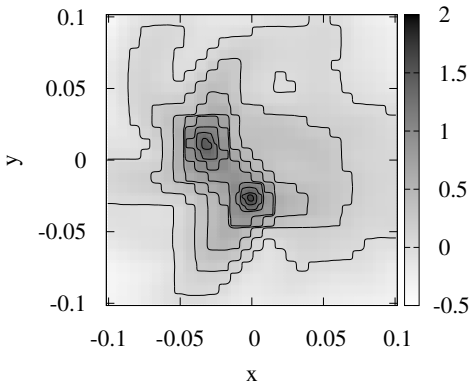


Figure 1 The final spatial distribution of $\log_{10}$ of column density along initial rotation axis in the model with $\varepsilon_{\rm T} = 0.3$, $\varepsilon_{\Omega} = 0.1$, $\varepsilon_{\rm M} = 0.2$, $\varepsilon_{\rm tk} = 0.2$.

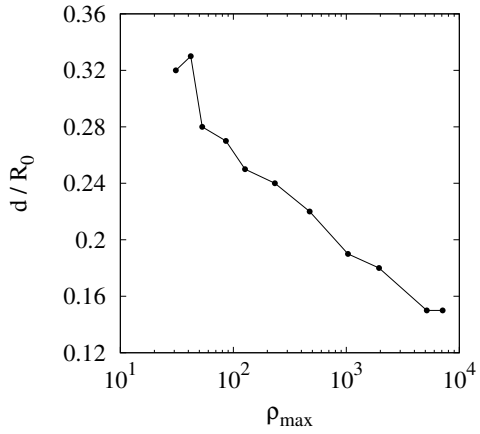


Figure 2 The ratio of separation between fragments to initial cloud radius as the function of maximal density in the model with $\varepsilon_{\rm T} = 0.3$, $\varepsilon_{\Omega} = 0.1$, $\varepsilon_{\rm M} = 0.2$, $\varepsilon_{\rm tk} = 0.2$.

Only 36 of 103 simulations demonstrated fragmentation. Figure 1 shows the final distribution of $\log_{10}$ of column density along initial rotation axis in the model with $\varepsilon_{\rm T} = 0.3$, $\varepsilon_{\Omega} = 0.1$, $\varepsilon_{\rm M} = 0.2$, $\varepsilon_{\rm tk} = 0.2$, and Fig. 2 shows the evolution of separation between fragments in this model. The separation decreases during the cloud collapse because of large scale inward motion.

Table 2 shows final fragments masses (relative initial cloud mass) and separations between fragments (relative initial cloud radius) in 4 groups of models. In every group the thermal and magnetic parameters ($\varepsilon_{\rm T}$ and $\varepsilon_{\rm M}$) are fixed while the rotational and turbulent parameters (ε_{Ω} and $\varepsilon_{\rm tk}$) are changed. The realizations of initial turbulence can be different also.

Analysis of Table 2 reveals the positive correlations between fragments separation and the sum $\varepsilon_{\Omega}+\varepsilon_{\rm tk}$. However, in models with $\varepsilon_{\Omega}+\varepsilon_{\rm tk} = 0.1$ fragmentation happened only in weakly magnetized case ($\varepsilon_{\rm M} = 0.01$), due to inefficient removing of angular momentum by MHD waves from the cloud center. For this reason, the models 1b1, 1b2 and 1c demonstrated the origin of triple systems with separations up to $0.39R_0$!

Model 4f does not show fragmentation because of casual neutralization of cloud rotation by velocity pulsations in the central region where magnetosonic waves become gravitationally unstable. This effect is also responsible for the absence of fragmentation in 6 of 7 variants of model 4b, and in 5 of 7 variants of model 4d.

4 Conclusion

Modeling the collapse and fragmentation of rotating turbulent protostellar clouds with the help of 3D MHD numerical code Megalion with AMR technology, we point out the obstacle of early cloud fragmentation. We found that fragmentation occurs only in part of runs, e.g. in 2 runs from 7. It is because turbulent velocity pulsations are directed randomly relative cloud rotation velocity. Only in some cases the turbulent and rotational velocities in cloud central part are codirectional. In these cases the

Table 2 Model parameters and results. $\varepsilon_{\rm T}$, ε_{Ω}, $\varepsilon_{\rm M}$, $\varepsilon_{\rm tk}$ are the initial ratios of thermal, rotational, magnetic and turbulent kinetic energies to the absolute value of gravitational energy of the cloud. m/M is the final fragment-to-cloud mass ratio, d/R_0 is the final ratio of fragments separation to initial cloud radius. The first digit in the model name marks the pair $\varepsilon_{\rm T}$ and $\varepsilon_{\rm M}$, the letter marks the pair ε_{Ω} and $\varepsilon_{\rm tk}$, the second digit is the variant of turbulence realization.

Name	$\varepsilon_{\rm T}$	ε_{Ω}	$\varepsilon_{\rm M}$	$\varepsilon_{\rm tk}$	m/M	d/R_0
1a	0.15	0	0.01	0.1	0.024, 0.008	0.04
1b0	0.15	0.1	0.01	0.01	0.088, 0.031	0.15
1b1	0.15	0.1	0.01	0.01	0.009, 0.008, 0.008	0.20, 0.39, 0.22
1b2	0.15	0.1	0.01	0.01	0.048, 0.016, 0.010	0.32, 0.34, 0.20
1c	0.15	0.1	0.01	0.1	0.060, 0.010, 0.008	0.30, 0.29, 0.10
2a	0.15	0.05	0.1	0.1	0.029, 0.009	0.14
2b	0.15	0.1	0.1	0.05	0.034, 0.031	0.15
2c0	0.15	0.1	0.1	0.1	0.037, 0.025	0.17
2c3	0.15	0.1	0.1	0.1	0.025, 0.022	0.16
3a	0.15	0	0.3	0.1	no fragmentation	–
3b2	0.15	0	0.3	0.3	0.054, 0.018	0.17
3c	0.15	0.1	0.3	0.1	0.047, 0.042	0.22
3d	0.15	0.1	0.3	0.2	0.068, 0.052	0.26
4a	0.3	0	0.2	0.1	no fragmentation	–
4b	0.3	0.05	0.2	0.1	0.038, 0.037	0.13
4c	0.3	0.05	0.2	0.2	0.049, 0.042	0.09
4d0	0.3	0.1	0.2	0.1	0.064, 0.059	0.16
4d4	0.3	0.1	0.2	0.1	0.057, 0.028	0.10
4e	0.3	0.1	0.2	0.2	0.078, 0.061	0.15
4f	0.3	0.1	0.2	0.5	no fragmentation	–
4g	0.3	0.2	0.2	0.4	0.1, 0.09	0.31

ratio of rotational to gravitational energies is large enough to cloud fragmentation at isothermal stage of collapse and the formation of very wide binaries.

Our results confirm the idea that protostellar clouds fragmentation is the main formation mechanism both of close and wide binary stars.

Acknowledgements The work is partially supported by grant "The foundation of perspective research" of Chelyabinsk State University in 2016.

References

Allen C., Monroy-Rodriguez M.A. (2014) ApJ 790, 158
Brandner W., Kohler R. (1998) ApJ 499, L79
Burzle F., Clark P.C., Stasyszyn F. et al. (2011) MNRAS 412, 171
Chen X., Arce H.G., Zhang Q. et al. (2013) ApJ 768, 110
Connelley M.S., Reipurth Bo, Tokunaga A.T. (2008) AJ 135, 2526
Dudorov A.E., Zhilkin A.G., Kuznetsov O.A. (1999) Matem. Mod. 11, 101 (in Russian)

Dudorov A.E., Zhilkin A.G., Stepanov K.E. et al. (2003) in: VII Zababakhin Scientific Talks, Int. Conf. Proc., http://www.vniitf.ru/rig/konfer/7zst/reports/s6/s-6.htm (in Russian)
Dudorov A.E. and Zamozdra S.N. (2012) in: XI Zababakhin Scientific Talks, Int. Conf. Proc., http://www.vniitf.ru/images/zst/2012/s3/3-14.pdf (in Russian)
Dudorov A.E., Zamozdra S.N. (2013) A&AT 28, 27
Hincelin U., Commercon B., Wakelam V. et al. (2016) ApJ 822, 12
Hunter J.H. (1979) ApJ 233, 946
Joos M., Hennebelle P., Ciardi A., Fromang S. (2013) A&A 554, A17
Kaib N.A., Raymond S.N. (2014) ApJ 782, 60
Kouwenhoven M. B. N. et al. (2009) in: Star clusters: basic galactic building blocks (IAU Symp. 266), eds. R. de Grijs and J. R. D. Lepine, p. 438
Kraus A.L., Hillenbrand L.A. (2009) ApJ 703, 1511
Longhitano M., Binggeli B. (2010) A&A 509A, 46L
Raghavan D., McAlister H.A., Henry T.J. et al. (2010) ApJSS 190, 1
Scholz R.-D., Kharchenko N.V., Lodieu N., McCaughrean M.J. (2008) A&A 487, 595
Zinnecker H. (1984) Ap&SS 99, 41